SCIENTIFIC REPORTS

OPEN

Thermal and impact histories of 25143 Itokawa recorded in Hayabusa particles

Received: 2 May 2018
Accepted: 23 July 2018
Published online: 07 August 2018

K. Terada[1], Y. Sano[2], N. Takahata[2], A. Ishida[3], A. Tsuchiyama[4], T. Nakamura[3], T. Noguchi[5], Y. Karouji[6], M. Uesugi[7], T. Yada[6], M. Nakabayashi[1], K. Fukuda[8,9] & H. Nagahara[8]

Understanding the origin and evolution of near-Earth asteroids (NEAs) is an issue of scientific interest and practical importance because NEAs are potentially hazardous to the Earth. However, when and how NEAs formed and their evolutionary history remain enigmas. Here, we report the U-Pb systematics of Itokawa particles for the first time. Ion microprobe analyses of seven phosphate grains from a single particle provide an isochron age of 4.64 ± 0.18 billion years (1σ). This ancient phosphate age is thought to represent the thermal metamorphism of Itokawa's parent body, which is identical to that of typical LL chondrites. In addition, the incorporation of other particles suggests that a significant shock event might have occurred 1.51 ± 0.85 billion years ago (1σ), which is significantly different from the shock ages of 4.2 billion years of the majority of shocked LL chondrites and similar to that of the Chelyabinsk meteorite. Combining these data with recent Ar-Ar studies on particles from a different landing site, we conclude that a globally intense impact, possibly a catastrophic event, occurred ca. 1.4 Ga ago. This conclusion enables us to establish constraints on the timescale of asteroid disruption frequency, the validity of the crater chronology and the mean lifetime of small NEAs.

A long-standing issue in planetary science is the connection between individual meteorites and their asteroidal parent bodies. Based on telescopic observation, one of the largest groups of asteroids (S-type) was found to have a mineralogy (low-calcium pyroxene and olivine) similar to that of the most common class of meteorites (80%, ordinary chondrites)[1]. Recent visible and infrared spectroscopic measurements suggest that most S-type NEAs, including Itokawa, exhibit possible links to LL ordinary chondrites[2–4]. However, until the Hayabusa sample return mission, there was no direct evidence of a connection between meteorites and asteroids except the observed fall of Almahata Sitta, which provided a link between an F-type asteroid (2008 TC3) and dark carbon-rich anomalous ureilites[5].

The Hayabusa sample-return mission was designed to explore a small S-type NEA, 25143 Itokawa, and has provided many insights into the properties of tiny "rubble-pile" NEAs (references in[6]). The initial comprehensive studies on the mineralogy, petrology, geochemistry and morphology of the regolith particles recovered from the Itokawa surface revealed that the particles consist of the same minerals as those that comprise LL5-6 chondrites (references in[7]). Based on two-pyroxene and/or olivine-spinel geothermometries, Nakamura *et al.*[7] showed that the highly equilibrated particles experienced a peak metamorphic temperature of ~800 °C and cooled slowly to 600 °C. Since temperatures of thermal metamorphism in asteroids increase with depth, the observed maximum temperature of 800 °C and the slow cooling rate require a diameter of the original asteroid larger than 20 km, possibly with an onion-shell structure, such as the H chondrite parent body[8]. After this intense thermal metamorphism and the subsequent cooling, it is considered that the Itokawa parent body was catastrophically disaggregated by one or multiple impacts into numerous small pieces, some of which re-accreted into the present greatly diminished, rubble-pile asteroid[6,7].

[1]Graduate School of Science, Osaka University, Toyonaka, 560-0043, Japan. [2]Atmosphere and Ocean Research Institute, The University of Tokyo, Chiba, 277-8564, Japan. [3]Graduate School of Science, Tohoku University, Sendai, 980-8578, Japan. [4]Graduate School of Science, Kyoto University, Kyoto, 606-8502, Japan. [5]Faculty of Arts and Science, Kyushu University, Fukuoka, 819-0395, Japan. [6]JAXA, Sagamihara, 252-5210, Japan. [7]JASRI/SPring-8, Hyogo, 679-5198, Japan. [8]Graduate School of Science, The University of Tokyo, Bunkyo-ku, 113-0033, Japan. [9]Department of Geoscience, University of Wisconsin-Madison, Wisconsin, 53706, USA. Correspondence and requests for materials should be addressed to K.T. (email: terada@ess.sci.osaka-u.ac.jp)

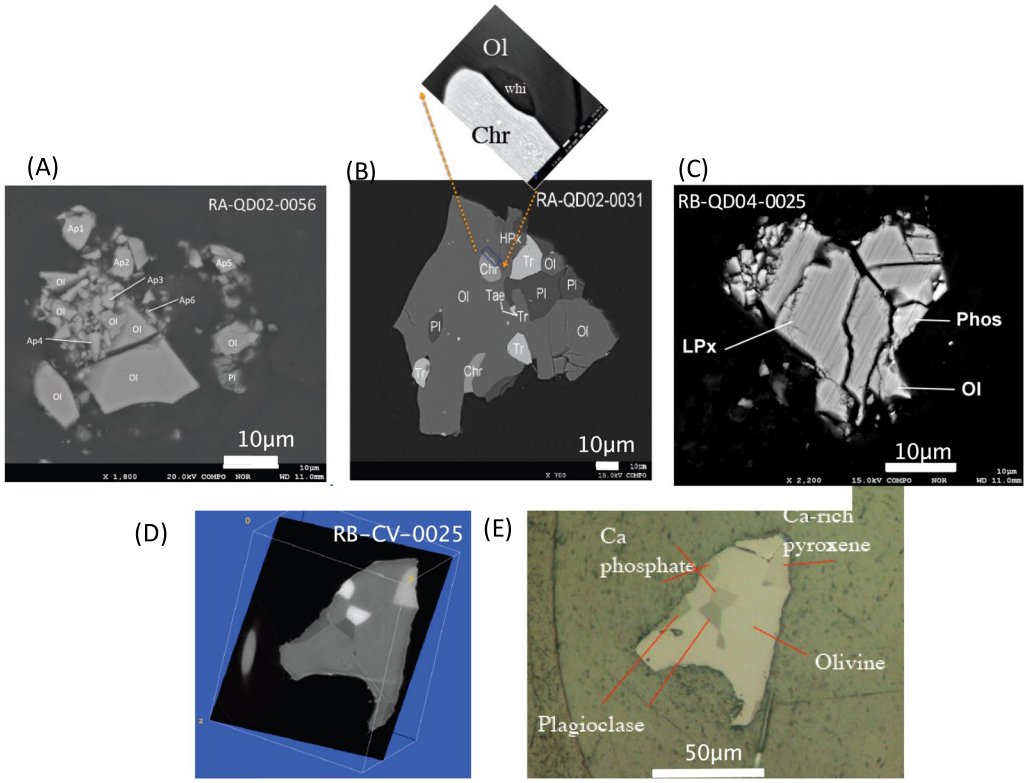

Figure 1. Back-scattered electron images of the Itokawa particles. (**A**–**C**) Show back-scattered images of polished sections of RA-QD02-0056, RA-QD02-0031, RB-QD04-0025, respectively. (**D**) Shows the "simulated" slice image of RB-CV-0025 before polishing, based on X-ray microtomography. Here, the angle and depth are selected where the cross sections inside two phosphates become the largest. (**E**) Shows the "actual" microscope image after careful manual polishing. Most phosphate grains are on the order of 2 μm × 4 μm to 4 μm × 5 μm in size.

Results

To better understand the thermal and impact histories of Itokawa, we investigated the U-Pb systematics of phosphate minerals in Itokawa regolith particles using an ion microprobe. Generally, phosphates are the primary carriers of U in ordinary chondrites and resistant to secondary thermal events due to their relatively high closure temperatures of 500–600 °C for Pb. One of the great advantages of U-Pb systematics is that there are two U decay series (^{238}U-^{206}Pb and ^{235}U-^{207}Pb), which potentially provides chronological information of not only a crystallization age but also an alteration age[9,10]. In this study, we adopt an advanced total Pb/U isochron method in the ^{238}U/^{206}Pb - ^{207}Pb/^{206}Pb - ^{204}Pb/^{206}Pb 3-D space for an improved age calibration from an obtained U-Pb data set. Cogenetic samples with an undistributed U-Pb system that share the same common-Pb isotopic composition must define a LINE in the ^{238}U/^{206}Pb - ^{207}Pb/^{206}Pb - ^{204}Pb/^{206}Pb space, whose intersection with the U-Pb concordia curve on the ^{238}U/^{206}Pb - ^{207}Pb/^{206}Pb plane provides a formation age. In contrast, for the discordia case, the plotted data in 3-D space are expressed by PLANAR regression. In this case, the upper and lower intercepts with the U-Pb concordia curve correspond to a formation age and an alteration age, respectively. We have demonstrated the robustness of our U-Pb *in situ* dating technique for various meteorites (references in[10]).

Figure 1(A–C) show back-scattered images of allocated polished sections of RA-QD02-0056, RA-QD02-0031, RB-QD04-0025, respectively. For these grains, the phosphate locations are well confirmed based on SEM-EDS analysis. However, RB-CV-0025 was an entire particle (i.e., not polished) when the sample was allocated, although an analytical dual-energy X-ray microtomography[11] suggests the occurrence of phosphates in the particle. Figure 1(D) shows the "simulated" slice image of the particle based on X-ray microtomography, where the cross sections inside two internal phosphates become as large as possible. Figure 1(E) shows the "actual" microscope image after careful manual polishing. RA-QD02-0031, RB-QD04-0025 and RB-CV-0025 exhibit a crystalline texture primarily consisting of olivine, plagioclase, chromite, pyroxene and troilite, with the accessary minerals taenite and whitlockite. In contrast, RA-QD02-0056 displays a brecciated texture and consists of olivine and plagioclase with several apatite grains. This particle is so fragile that there was no possibility of surviving the severe shock after compaction, which is well demonstrated by the fact that RA-QD02-0056 was split into small particles at the time of embedding in the epoxy resin. Most phosphate grains are from 2 μm × 4 μm to 5 μm × 7 μm in size. The chemical compositions of the phosphates are listed in Table 1. Based on the combination of two-pyroxene geothermometers, RA-QD02-0031 is an equilibrated particle that experienced a peak metamorphic temperature of 799 ± 16 °C. Although RA-QD02-0056 does not include two-pyroxenes, an Fa number for olivine of 29.6 ± 0.3 (n = 8) suggests that it is an equilibrium particle[7]. In previous studies, oxygen isotope measurements

Grain No.	RA-QD02-0056	RA-QD02-0056	RA-QD02-0056	RA-QD02-0031	RB-CV-0025	RB-CV-0025	RB-QD04-0025
Spot No.	1	2	3	1	1	2	1
SiO_2	0.29	1.48	2.40	0.26	3.59	0.37	3.756
TiO_2	0.06	n.d.	n.d.	n.d.	0.08	0.15	n.d.
Al_2O_3	n.d.	n.d.	n.d.	0.01	0.03	0.14	n.d.
FeO	0.10	0.26	1.12	1.18	n.d.	n.d.	2.592
MnO	n.d.	0.02	0.04	0.04	n.d.	n.d.	0.04
MgO	n.d.	0.47	2.13	3.56	7.58	4.02	7.79
CaO	55.60	53.12	50.67	42.31	40.53	45.36	40.871
Na_2O	0.36	0.38	0.35	2.53	1.45	2.11	2.51
K_2O	n.d.	0.03	0.02	0.07	n.d.	n.d.	0.049
Cr_2O_3	n.d.	n.d.	0.02	0.44	n.d.	n.d.	n.d.
NiO	0.02	n.d.	0.02	n.d.	n.d.	n.d.	n.d.
P_2O_5	42.80	40.11	38.67	42.69	37.32	42.32	39.589
SO_3	0.07	0.11	0.04	0.06	0.01	0.01	n.d.
Cl	5.54	3.65	3.68	—	9.39	5.53	0.226
Total	103.59	99.45	98.66	93.15	99.98	100.01	97.382

Table 1. Chemical composition of typical phosphate grains.

Grain No.	Spot No.	Mineral	U (p.p.m.)	$^{238}U/^{206}Pb$	$^{207}Pb/^{206}Pb$	$^{204}Pb/^{206}Pb$
RA-QD02-0056	0717_1	apatite	2.9	0.2405 ± 0.0310	0.8144 ± 0.0839	0.0270 ± 0.0079
RA-QD02-0056	0717_4	apatite	2.9	0.4241 ± 0.1913	0.8149 ± 0.1572	0.1251 ± 0.0487
RA-QD02-0056	0718_1	apatite	4.0	0.1809 ± 0.0216	0.7917 ± 0.0815	0.0298 ± 0.0073
RA-QD02-0056	0718_2	apatite	4.0	0.2878 ± 0.0859	0.7016 ± 0.2542	0.0302 ± 0.0340
RA-QD02-0056	0718_3	apatite	3.7	0.8375 ± 0.1959	0.6527 ± 0.0830	0.0007 ± 0.0022
RA-QD02-0056	0718_5	apatite	6.6	0.3992 ± 0.1080	0.6545 ± 0.1797	0.0128 ± 0.0179
RA-QD02-0031	0717_3	whitlockite	0.047	0.0266 ± 0.1047	1.0000 ± 1.0092	0.1133 ± 0.1931
RB-CV-0025	1218_1	whitlockite	0.201	0.6720 ± 0.2970	0.7690 ± 0.3380	0.0385 ± 0.0392
RB-CV-0025	1218_2	whitlockite	0.240	0.5760 ± 0.2710	0.6920 ± 0.5410	0.1540 ± 0.1170
RB-QD04-0025	0811_3	whitlockite	0.123	1.3301 ± 0.3132	0.6038 ± 0.1052	0.0755 ± 0.0391
RB-QD04-0025	0812_1	whitlockite	0.282	0.8570 ± 0.5160	0.7500 ± 0.1164	0.0357 ± 0.0263
from Göpel *et al.*[13]						
St. Severin (LL6)			0.44	0.96021 ± 0.02528	0.63590 ± 0.00041	0.00370 ± 0.00007
Guidder (LL5)			0.23	0.97578 ± 0.17499	0.61456 ± 0.00047	0.00069 ± 0.00009
Tuxtuac (LL5)			0.42	0.96693 ± 0.10284	0.62380 ± 0.00100	0.00195 ± 0.00014

Table 2. Isotope ratios in phosphates for Itokawa particles and unshocked LL chondrites.

of olivine for both grains and the shock stage for RA-QD02-0031 have been investigated and exhibit similarity to less shocked LL chondrites[7,12]. Interestingly, it has been confirmed by TEM observation that RA-QD02-0056 consists of mineral grains whose surface has a thin layer (0–15 nm) induced by space weathering. Thus, the constituents of RA-QD02-0056 might have been individual particles before they formed a single grain possibly due to compaction.

An ion microprobe study was performed on phosphates in four Itokawa particles with NanoSIMS at the University of Tokyo. The data are shown in Table 2. The large uncertainties of the individual data points are due to low counting rates. Specifically, data point #0031-01 (whitlockite) shows a large uncertainty because this grain is a particularly small whitlockite whose U concentration is extremely low (less than one-tenth that of apatite). The U-Pb systematics of a single particle (RA-QD02-0056) reveal it to be concordant, providing a total Pb/U isochron age of 4.64 ± 0.18 Ga (1σ) in the $^{238}U/^{206}Pb$ - $^{207}Pb/^{206}Pb$ - $^{204}Pb/^{206}Pb$ 3-D space (Fig. 2(A)). This outcome represents the first reported thermal metamorphism age of Itokawa particles. This age is identical to that of typical LL5 and LL6 chondrites (4.54–4.56 Ga)[13,14]. Although analytical uncertainty regarding the obtained U-Pb age is large, that ^{26}Mg–excess was not observed in Itokawa particles[15] suggests that thermal metamorphism continued for several million years (until ^{26}Al decayed) after the CAI formation. The U-Pb systematics of RA-QD02-0031, which was not exposed to a severe shock (S2[12] and/or up to S4[7]), are also consistent with those of RA-QD02-0056 within the analytical uncertainty. However, two other particles (RB−QD04-0025 and RB-CV-0025) exhibit discordant U-Pb systematics. Therefore, the combined U-Pb data of the four particles are NOT expressed by a linear regression in 3-D space but are well expressed by a planar regression (Y = −0.19X + 0.82 + 0.37Z), providing an upper intersection age of 4.58 ± 0.31 Ga and a lower intersection age of 1.51± 0.85 Ga (1σ) (Fig. 2(B)).

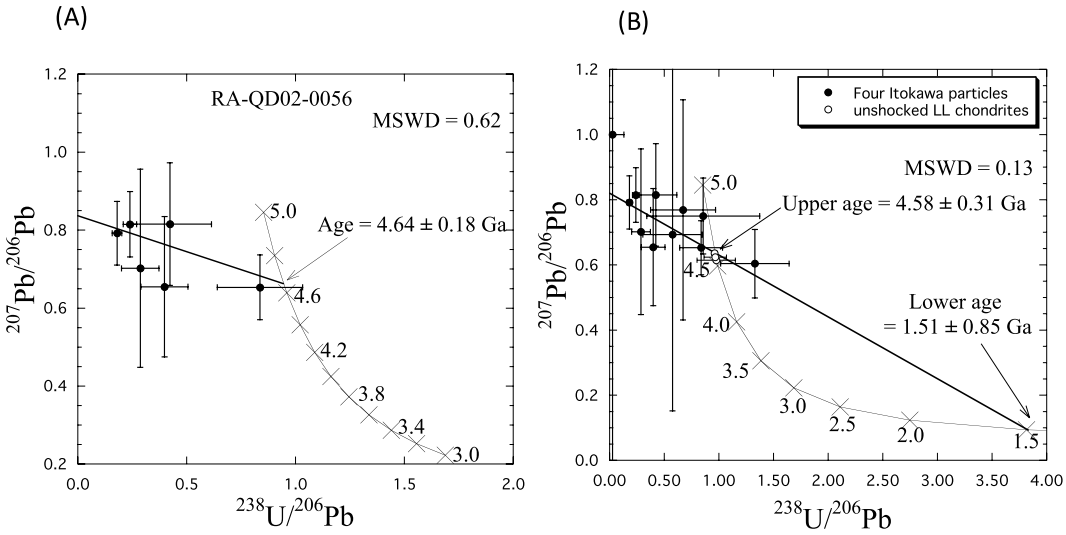

Figure 2. Result of *in situ* U-Pb dating of phosphates in Itokawa particles. The diagram projected onto the $^{238}U/^{206}Pb$ - $^{207}Pb/^{206}Pb$ plane of the total Pb/U isochron in three-dimensional $^{238}U/^{206}Pb$ - $^{207}Pb/^{206}Pb$ - $^{204}Pb/^{206}Pb$ space for a single particle (RA-QD02-0056) (**A**) and four particles (**B**), respectively. For comparison, the data for unshocked LL chondrites are shown in (**B**). The uncertainties of the plotted data and obtained ages are reported at the 1 sigma level. All data suggest that the crystallization ages of the Itokawa phosphates are approximately 4.6 Ga. U-Pb systematics of four Itokawa particles are well expressed by a planar regression in the 3-D space, providing an upper intersection age of 4.58 ± 0.31 Ga and a lower intersection age of 1.51 ± 0.85 Ga (1σ) with the concordia line on the $^{238}U/^{206}Pb$ - $^{207}Pb/^{206}Pb$ plane. These ages are thought to be a thermal metamorphism age and a shock age, respectively. The linear regression (**A**) and planar regression (**B**) were calibrated using Isoplot/Ex.

These outcomes are thought to be vestiges of a thermal metamorphism age and a shock age recorded in Itokawa particles, respectively. The younger age of 1.51 ± 0.85 Ga is consistent with Ar-Ar ages of $(1.3–1.4) \pm 0.3$ Ga for three Itokawa particles[16] but different from the Ar-Ar age of 2.3 ± 0.1 Ga for the single grain[17]. It should be noted that the U-Pb system is highly resistant to secondary events in contrast to the Ar-Ar system, which is sensitive to shock. Therefore, the observed U-Pb disturbance of Itokawa particles and the consistency of Ar-Ar ages of particles collected from a different landing site provide robust evidence that a cataclysmic/catastrophic impact event occurred on the Itokawa parent body 1.4 billion years ago (which is the weighted mean of the U-Pb discordant age and the Ar-Ar plateau age[16]), causing the disruption of the parent body of the Itokawa. Although the mineralogy and geochemistry of the Itokawa particles resemble those of LL chondrites[7], this cataclysmic impact age differs from the Ar-Ar ages of most shocked LL chondrites, which exhibit a peak at approximately 4.2 Ga and no indication at approximately 1.3–1.4 Ga[18–20]. Considering the sensitivity of Ar-Ar ages to shock events, we conclude that Itokawa has experienced an evolutionary history different from that of most LL chondrites. However, certain LL chondrites, including the Chelyabinsk meteorite, exhibit evidence of a similar event near 1.5 Ga[21]. It is interesting to note that the Chelyabinsk meteorite is derived from the Flora and Baptistina asteroid families[22] and that the estimated dispersion age of the Flora family (950 ± 200 Myr)[23] is marginally consistent with our chronological records (1.51 ± 0.85 Ga for the U-Pb age and $(1.3–1.4) \pm 0.3$ Ga for the Ar-Ar ages).

Discussion

Numerous chronological studies have been performed on S-type NEAs. Gladman *et al.*[24] estimated the median lifetime of such NEAs to be ~10 Myr (up to 60 Myr). These NEAs terminate by striking a terrestrial planet (10–30% of NEAs), entering a Sun-grazing state (more than half) or escaping from the Solar System (approximately 15%). That NEAs exist in the vicinity of Earth suggests a continuous supply from the main belt to maintain the population of these objects with very short lifetimes compared to the age of the Solar System. Michel and Yoshikawa[25] pointed out that most S-type NEAs, including Itokawa, likely originate in the inner main belt through the $\nu 6$ secular resonance. The dynamical time required to become an Earth-crosser through such a strong main belt resonance is estimated to be only a few million years[26]. In contrast, Bottke *et al.*[27] reported asteroid disruption frequency in the main belt of once every billion years for objects >100 km and 15–30 times per billion years for objects 25–35 km in diameter. According to N-body calculations, the gravitational re-accumulation time after a collision is very short (typically several days)[28]. Using another approach, O'Brien *et al.*[29] investigated the crater size distribution on the surface of several S-type asteroids observed at high spatial resolution by a spacecraft and reported 1 billion years for Gaspra (10–20 km size), 0.5–1 billion years for Ida (20–60 km size), and 1.2 million years for Eros (11–34 km). It should be noted that Gaspra and Ida lie in the main belt, but Eros is an NEA. Michel *et al.*[30] recently suggested that the time required to accumulate Itokawa's craters was at least 75 million years and maybe up to 1 billion years, depending on the applied scaling law. Tatsumi *et al.*[31] also suggested a crater retention age of 3–33 Myr based on more realistic collision experiments[31]. Taking the probable size of the parent body

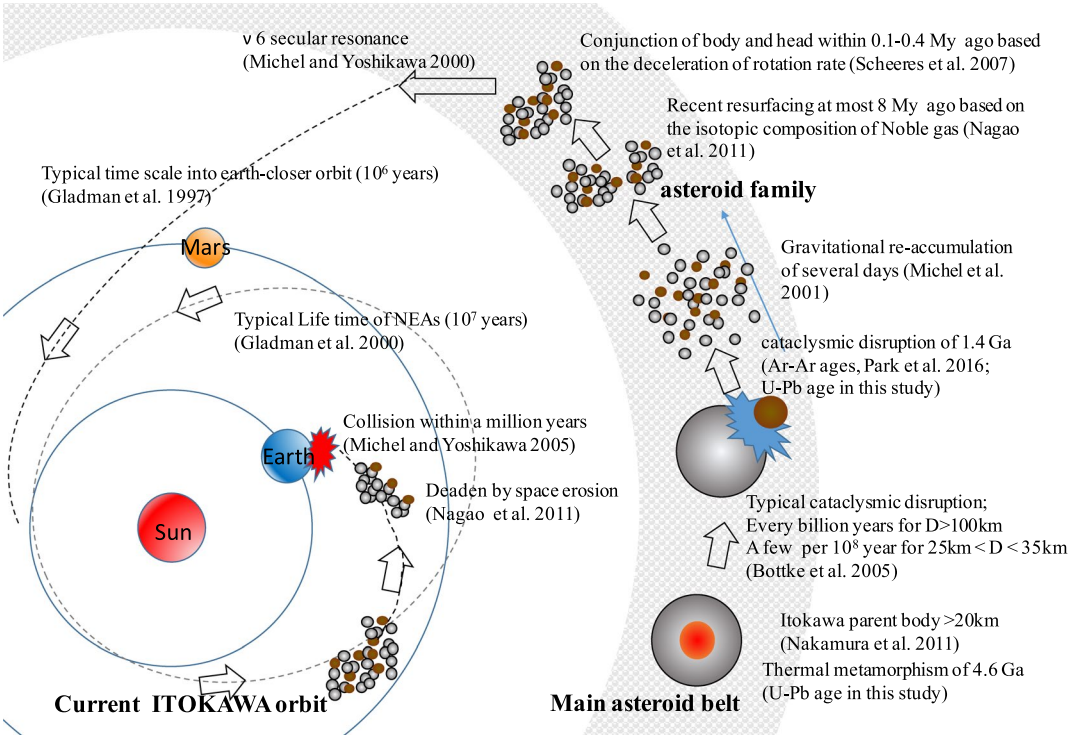

Figure 3. Overview of time evolution of the Itokawa asteroid. This illustration summarizes the various chronological data reported for the Itokawa asteroid, including evident radiometrical ages, the estimated timescale of N-body simulation and modelling based on the deceleration of the rotation rate (see text for details).

of Itokawa (>20 km[7]) and/or LL chondrites (10–50 km[14]) into consideration, we can state that our radiometric impact age of 1.36 ± 0.24 Ga is approximately consistent with the timescale of asteroid collision frequency in the main belt and the crater chronology of S-type asteroids in the main belt and slightly longer than the crater age of Itokawa. This outcome may be the result of global resurfacing that resets the 1–10 m deep surface layer, which may have occurred in the main belt long after the possible catastrophic disruption of the rigid parent of Itokawa[31]. The short residence time of Itokawa particles (less than 8 Myrs), implied by estimation from cosmic-ray-produced ^{22}Ne, also supports the recent resurfacing scenario (losing/cultivating its surface materials at a rate of approximately 10 m per 10^8 years)[32].

The observation of a deceleration in the rotation rate of Itokawa also constrains Itokawa's evolution to within the last 0.1–0.4 million years during which period the conjunction of the two parts referred to as "head" and "body" by a low velocity impact occurred[33]. This conjunction must have occurred after the disruption event and the subsequent main re-accumulation and possibly while the Itokawa fragments still resided within the main belt. Combining our results with those of other theoretical studies, we propose that an intense impact event on Itokawa's parent body (possibly catastrophic disruption) and reassembly occurred within the asteroid main belt and that its by-product, Itokawa, must have spent on the order of thousands of million years in the main belt. This period probably continued after the conjunction of the "head" and "body", which belong to the "family", within the last 0.1–0.4 million years. Then, Itokawa was injected into its current Earth-crossing orbit via the ν6 resonance. In addition, we predict that Itokawa will collide with the Earth within a million years[34] and/or be destroyed by space erosion[32]. These chronological inferences for the Itokawa asteroid are summarized in Fig. 3.

Finally, we emphasize that our successful chronology results for Itokawa are based on a single brecciated particle, RA-QD02–0056, that includes several apatite grains. Such a brecciated grain is so fragile that it may not have been collected if the Hayabusa spacecraft sampling mechanism had operated as planned and its impactors struck the Itokawa surface. Fortunately, because the Hayabusa curation team found other particles that may include phosphorous minerals, further ion microprobe studies on the U-Pb systematics will place tighter constraints on local and global impact ages on Itokawa and clearly determine the time evolution of the typical small NEA Itokawa.

Materials and Methods

Three polished sections of Itokawa particles (RA-QD02-0056, RA-QD02-0031, RB-QD04-0025) and one entire grain (RB-CV-0025) were provided by the Planetary Material Sample Curation Facility of JAXA (PMSCF/JAXA). For RB-CV-0025, analytical dual-energy X-ray microtomography[11] suggested the occurrence of phosphates in the particle. Figure 1(D) shows the "simulated" slice image of the particle based on X-ray microtomography in which the cross sections inside two internal phosphates become as large as possible. Figure 1(E) shows the "actual" microscope image after careful manual polishing. After observation using a field emission scanning electron

Magnet field	EM1	EM2	EM3	EM4	EM5
B1			$^{204}Pb^{+}$		
B2	$^{44}Ca^{+}$		$^{206}Pb^{+}$	$^{238}U^{16}O^{+}$	$^{238}U^{16}O_2^{+}$
B3			$^{207}Pb^{+}$		

Table 3. Run table of U-Pb dating for phosphates.

microscope at Kyoto University, the polished sections were gold-coated to prevent charging of the sample surface during NanoSIMS analyses. To further reduce the already very small $^{x-1}PbH^{+}$ interference on the $^{x}Pb^{+}$ peaks, the samples were baked and evacuated in the preload chamber overnight. In an important final step before the actual analysis, rastering of the primary ion beam over the sample surface for 5 minutes was performed to remove any remaining contaminants.

For *in situ* U–Pb dating, we used a NanoSIMS installed at the University of Tokyo, Japan. A 0.1 nA O^{-} primary beam with an acceleration voltage of 16 kV was focused to 1 μm and used to map an area of 2 μm × 2 μm to 5 μm × 5 μm by 32 pixels × 32 pixels depending on phosphate grain size. Then, positive secondary ions ($^{44}Ca^{+}$, $^{204}Pb^{+}$, $^{206}Pb^{+}$, $^{207}Pb^{+}$, $^{238}U^{16}O^{+}$, $^{238}U^{16}O_2^{+}$) were extracted and detected using the 5-Electron Multiplier (EM) system by 3-step magnetic-field switching as follows. In the first step, $^{204}Pb^{+}$ ions were measured by a single collector. Then, $^{44}Ca^{+}$, $^{206}Pb^{+}$, $^{238}U^{16}O^{+}$, $^{238}U^{16}O_2^{+}$ ions were simultaneously collected by four detectors. Finally $^{207}Pb^{+}$ ions were measured by a single collector. The run tables of U-Pb dating in this study are listed in Table 3. One analysis session lasted approximately 180 minutes while switching the magnetic field (1 minute accumulation * 3 magnet steps * 60 cycles). The mass resolution was set at approximately 4200 at ^{206}Pb (10% peak height), which is sufficient to separate Pb peaks from any interference peaks. A typical background is a few counts per 60 minutes per detector.

Since these mapping areas are comparable and/or slightly larger than the actual grain size, we extracted the appropriate pixels from the mapping area, in which the ^{44}Ca ion counts are larger than 90% of those of standard apatite, and accumulated secondary ion counts of these appropriate pixels. The mass resolution was set to approximately 4200 at ^{206}Pb for the U–Pb analyses.

The abundance ratios of ^{238}U to ^{206}Pb for phosphates were calibrated from the observed $^{238}UO^{+}/^{206}Pb^{+}$ ratios using an empirical quadratic relationship between the $^{206}Pb^{+}/^{238}UO^{+}$ and $^{238}UO_2^{+}/^{238}UO^{+}$ ratios of standard apatite derived from an alkaline rock of the Prairie Lake circular complex in the Canadian Shield (1156 ± 45 Myr (2σ)[35]).

References

1. Binzel, R. P., Bus, S. J., Burbine, T. H. & Sunshine, J. M. Spectral Properties of Near-Earth Asteroids: Evidence for Sources of Ordinary Chondrite Meteorites. *Science* **273**, 946–948 (1996).
2. Binzel, R. P., Rivkin, A. S., Bus, S. J., Sunshine, J. M. & Burbine, T. H. MUSES-C target asteroid (25143) 1998 SF36: A reddened ordinary chondrite. *Meteoritics & Planetary Science* **36**, 1167–1172 (2001).
3. Vernazza, P. *et al*. Compositional differences between meteorites and near-Earth asteroids. *Nature* **454**, 858–860 (2008).
4. Dunn, T. L., Burbine, T. H., Bottke, W. F. & Clark, J. P. Mineralogies and source regions of near-Earth asteroids. *Icarus* **222**, 273–282 (2013).
5. Jenniskens, P. *et al*. The impact and recovery of asteroid 2008 TC_3. *Nature* **458**, 485–488 (2009).
6. Fujiwara, A. *et al*. The Rubble-Pile Asteroid Itokawa as Observed by Hayabusa. *Science* **312**, 1330–1334 (2006).
7. Nakamura, T. *et al*. Itokawa Dust Particles: A Direct Link Between S-Type Asteroids and Ordinary Chondrites. *Science* **333**, 1113–1116 (2011).
8. Trieloff, M. *et al*. Structure and thermal history of the H-chondrite parent asteroid revealed by thermochronometry. *Nature* **422**, 502–506 (2003).
9. Wendt., T. A three-dimensional U–Pb discordia plane to evaluate samples with common lead of unknown isotopic composition. *Chem. Geol.* **46**, 1–12 (1984).
10. Terada, K. & Sano, Y. *In-situ* U-Pb dating of apatite by Hiroshima-SHRIMP: Contributions to Earth and Planetary Science. *Mass Spectrometry* **1**, p.A0011 (2012).
11. Tsuchiyama, A. *et al*. Analytical dual-energy microtomography: A new method for obtaining three-dimensional mineral phase images and its application to Hayabusa samples. *Geochimica et Cosmochimica Acta* **116**, 5–16 (2014).
12. Zolensky, M. E. *et al*. The Shock State of Itokawa Samples. *LPSC* **XXXXIII**, #1659 (2012).
13. Göpel, C., Manhés, G. & Allégre, C. J. U-Pb systematics of phosphates from equilibrated ordinary chondrites. *Earth Planet. Sci. Lett.* **121**, 157–171 (1994).
14. Bouvier, A., Blichert-Toft, J., Moynier, F., Vervoort, J. D. & Albarède, F. Pb–Pb dating constraints on the accretion and cooling history of chondrites. *Geochimica et Cosmochimica Acta* **71**, 1583–1604 (2007).
15. Yurimoto H. *et al*. Oxygen and Magnesium Isotopic Compositions of Asteroid 25143 Itokawa Returned by the Hayabusa Mission. *Meteoritics and Planetary Science Supplement*, id.5320 (2011).
16. Park, J. *et al*. $^{40}Ar/^{39}Ar$ age of material returned from asteroid 25143 Itokawa. *Meteoritics and Planetary Science* **50**, 2087–2098 (2015).
17. Jourdan F *et al*. Collisional history of asteroid Itokawa. *Geology* **45**, 819–822 (2017).
18. Keil, K., Haack, H. & Scott, E. R. D. Catastrophic fragmentation of asteroids: Evidence from meteorites. *Planetary and Space Science* **42**, 1109–1122 (1994).
19. Dixon, E. T., Bogard, D. D., Garrison, D. H. & Rubin, A. E. 39Ar-40Ar evidence for early impact events on the LL parent body. *Geochimica et Cosmochimica Acta* **68**, 3779–3790 (2004).
20. Swindle T. D. & Kring D. A. Chronological evidence for the late heavy bombardment in ordinary chondrite meteorites. In: Workshop on Early Solar System Impact Bombardment, Lunar & Planetary Institute (abstract #3004) (2008).
21. Righter, K. *et al*. Mineralogy, petrology, chronology, and exposure history of the Chelyabinsk meteorite and parent body. *Meteoritics & Planetary Science* **50**, 1790–1819 (2015).
22. Reddy, V. *et al*. Chelyabinsk meteorite explains unusual spectral properties of Baptistina Asteroid Family. *Icarus* **237**, 116–130 (2014).

23. Dykhuis, M. J., Molnar, L., Van Kooten, S. J. & Greenberg, R. Defining the Flora Family: Orbital properties, reflectance properties and age. *Icarus* **243**, 111–128 (2014).
24. Gladman, B., Michel, P. & Froeschlé, C. The Near-Earth Object Population. *Icarus* **146**, 176–189 (2000).
25. Michel, P. & Yoshikawa, M. Dynamical origin of the asteroid (25143) Itokawa: the target of the sample-return Hayabusa space mission. *Astronomy and Astrophysics* **449**, 817–820 (2006).
26. Gladman, B. J. *et al*. Dynamical lifetimes of objects injected into asteroid belt resonances. *Science* **277**, 197–201 (1997).
27. Bottke, W. F. *et al*. The fossilized size distribution of the main asteroid belt. *Icarus* **175**, 111–140 (2005).
28. Michel, P., Benz, W., Tanga, P. & Richardson, D. C. Collisions and Gravitational Reaccumulation: Forming Asteroid Families and Satellites. *Science* **294**, 1696–1700 (2001).
29. O'Brien, D. P., Greenberg, R. & Richardson, J. E. Craters on asteroids: Reconciling diverse impact records with a common impacting population. *Icarus* **183**, 79–92 (2006).
30. Michel, P., O'Brien, D. P., Abe, S. & Hirata, N. Itokawa's cratering record as observed by Hayabusa: Implications for its age and collisional history. *Icarus* **200**, 503–513 (2009).
31. Tatsumi, E. & Sugita, S. Cratering efficiency on corase-grain targets: Implications for the dynamical evolution of asteroid 25143 Itokawa. *Icarus* **300**, 227–248 (2018).
32. Nagao, K. *et al*. Irradiation History of Itokawa Regolith Material Deduced from Noble Gases in the Hayabusa Samples. *Science* **333**, 1128–1131 (2011).
33. Scheeres, D. J. *et al*. The effect of YORP on Itokawa. *Icarus* **188**, 425–429 (2007).
34. Michel, P. & Yoshikawa, M. Earth impact probability of the Asteroid (25143) Itokawa to be sampled by the spacecraft Hayabusa. *Icarus* **179**, 291–296 (2005).
35. Sano, Y., Oyama, T., Terada, K. & Hidaka, H. Ion microprobe U-Pb dating of apatite. *Chem. Geol.* **153**, 249–258 (1999).

Acknowledgements

We thank Dr. Ludwig for furnishing the ISOPLOT/EX program used for U-Pb age calibration. This study was partially supported by a MEXT research fund (No. 17K18805).

Author Contributions

K.T. organized the research study and contributed to all of its aspects. Y.S. contributed the U-Pb dating using NanoSIMS. N.T. performed U-Pb analysis using NanoSIMS. A.I. also performed U-Pb analysis using NanoSIMS. A.T. performed the X-ray tomography. T.N. contributed to the SEM-EDS study. T.N. also contributed to the SEM-EDS study. Y.K. contributed to sample preparation and the SEM-EDS study. M.U. also contributed to sample preparation and the SEM-EDS study. T.Y. also contributed to sample preparation and the SEM-EDS study. M.N. performed U-Pb analysis and data calibration. K.F. contributed to U-Pb analysis using NanoSIS. H.N. contributed to the discussion.

Additional Information

Competing Interests: The authors declare no competing interests.

Publisher's note: Springer Nature remains neutral with regard to jurisdictional claims in published maps and institutional affiliations.